



Subtraction of time-resolved magnetic resonance angiography images improves visualization of the pulmonary veins and left atrium in adults with congenital heart disease: a novel post-processing technique

G. Sugrue¹ · A. Cradock² · A. McGee² · C. McEntee¹ · S. K. Eustace¹ · P. Fitzpatrick³ · L. P. Lawler¹ · J. G. Murray¹

Received: 23 January 2019 / Accepted: 15 March 2019 / Published online: 4 April 2019
© Springer Nature B.V. 2019

Abstract

To describe a novel time-resolved magnetic resonance angiography (TR-MRA) postprocessing technique using the time-resolved angiography with interleaved stochastic trajectories (TWIST) method to evaluate the pulmonary veins and left atrium in adults with congenital heart disease undergoing cardiac MRI. Institutional ethics committee approved the study. 21 consecutive adult patients (14 female, 7 male patients, mean age 28 years) with known congenital heart disease who underwent a cardiac MRI were included. Post-processing of the TR-MRA sequences created novel “subtracted” datasets. Two independent observers reviewed the conventional TWIST and novel subtracted TWIST data sets in source and maximum intensity projection (MIP) coronal reformats to assess visualization of the pulmonary veins and left atrium based on a 5-point scale. Quantitative signal to noise (SNR) comparison was performed. TR-MRA yielded diagnostic image data in 20/21 patients (95.2%). The novel “subtracted” TR-MRA technique improved visualization of the pulmonary veins and left atrium compared to the source TR-MRA sequence in 16/20 patients (mean scores 3.34 ± 0.69 vs. 2.92 ± 0.69 , $p < 0.008$). Further improved visualization of the pulmonary veins and left atrium was observed in the subtracted MIP TWIST sequences compared to the MIP TWIST images (mean scores 4.43 ± 0.80 vs. 3.02 ± 0.87 vs., $p < 0.001$). No significant SNR difference between the source and novel subtracted group was observed (85.4 vs. 70.4, $p = 0.57$). Compared to source TR-MRA images, subtraction of TR-MRA images is a novel postprocessing technique that improves visualization of the pulmonary veins and left atrium in a substantial number of patients.

Keywords Magnetic resonance angiography · Heart defects · Congenital · Pulmonary veins · Left atrium

Abbreviations

MRI Magnetic resonance imaging
CHD Congenital heart disease
MRA Magnetic resonance angiography

TWIST Time-resolved angiography with interleaved stochastic trajectories
RSPV Right superior pulmonary vein
LA Left atrium
ROI Region of interest
PA Pulmonary artery
MIP Maximum intensity projection
SI Signal intensity
SNR Signal-to-noise
TR-MRA Time resolved magnetic resonance angiography
CE-MRI Contrast enhanced magnetic resonance angiography

Electronic supplementary material The online version of this article (<https://doi.org/10.1007/s10554-019-01585-x>) contains supplementary material, which is available to authorized users.

✉ G. Sugrue
gavin.sugrue@vch.ca

¹ Department of Radiology, Mater Misericordiae University Hospital, Dublin, Ireland

² Radiography and Diagnostic Imaging, School of Medicine, University College Dublin, Belfield, Dublin 4, Ireland

³ School of Public Health, Physiotherapy & Sports Science, University College Dublin, Dublin, Ireland

Introduction

Contrast-enhanced cardiac magnetic resonance imaging (MRI) is a noninvasive tool used to evaluate anatomical, physiological and functional parameters in patients with congenital heart disease (CHD) [1, 2]. Significant advances in MRI hardware and imaging techniques, in particular time-resolved MRA techniques [3], now allow for assessment of the temporal dynamics of blood flow [4–6]. Due to complex hemodynamics, shunting and post-surgical anatomy, imaging patients with CHD poses unique challenges, in particular a difficulty with overlay of contrast in the arterial and pulmonary venous phases. Herein we describe a novel post-processing technique achieved by subtracting TWIST images in patients with complex CHD, and qualitatively and quantitatively assess image quality.

Materials and methods

Patients

The study was performed in agreement with the regulations of the local ethics committee. This was a prospective study of 21 consecutive adult patients over a 3 month period (June–August 2018) with known CHD. Indication for the investigation was based on clinical consideration by the referring cardiologist. One patient was excluded due to non-diagnostic imaging from significant motion artifact. Of the final cohort there were 14 males, 7 females; mean age 27 years with an age range 18–38 years. The spectrum of CHD included 11 (52.4%) patients with tetralogy of fallot, 6 (28.6%) with transposition of the great arteries, 1 (4.8%) Ebstein's anomaly, 1 (4.8%) pulmonary vein stenosis, 1 (4.8%) bicuspid aortic valve and 1 (4.8%) atrial septal defect (ASD). 17/21 (81.0%) patients had undergone prior corrective cardiac surgery.

Conventional MRI TWIST technique

MRI scans were performed on a 1.5T whole-body scanner (Magnetom Symphony with TIM Upgrade, Siemens, Erlangen, Germany) with the patient in a head-first supine position. A six-element receiver coil was used in association with the posterior spinal coil. A 20G plastic intravenous catheter was placed in the patient's antecubital vein for contrast administration. Our institutional standard cardiac MRI protocol was used for all patients including acquisition of half Fourier T2 weighted (HASTE), cine steady state free precession (cine True FISP), phase contrast imaging and 3D TWIST sequences. The TWIST sequence consists of

10 measurements. After the first pre-contrast breath hold measurement, a standardized 0.1 mmol/kg of gadobutrol (Gadovist; Bayer Pharma, Berlin, Germany) was injected at 3 ml/s, followed by a 20 ml saline flush at 3 ml/s. This was followed by acquisition of 9 consecutive breath hold measurements 4.0 s apart. The scan parameters for the TWIST sequence included a matrix of 512×358 , FOV $500 \text{ mm} \times 340 \text{ mm}$, voxel size $1.4 \times 1.0 \times 2.0 \text{ mm}^3$ and slice thickness of 2 mm. Slice resolution was 68.75%, TR/TE 2.87 ms/1.17 ms, flip angle 25° . 64 slices were acquired in the coronal orientation with an acquisition time of 41 s per data set. The source TWIST datasets included an automatic subtraction of the non-contrast “mask” image from the contrast enhanced data sets.

New subtraction technique

All images were archived on the picture archiving and communication system (PACS, McKesson, Canada). Manual subtraction of the data sets was performed by a MRI Radiographer on a dedicated post-processing workstation (Leonardo; Siemens Medical Solutions, Erlangen, Germany). A region of interest (ROI) was placed over the proximal right superior pulmonary vein (RSPV) and proximal right pulmonary artery (RPA) in all 9 consecutively acquired TWIST data sets to determine the data set that demonstrated peak opacification of the RSPV and the data set that demonstrated peak opacification of the RPA. The size of the region of interest (ROI) was standardized in all patients to cover 2/3 of the RPA and RSPV. These two anatomical landmarks were specifically chosen as representatives for the pulmonary venous and arterial systems. The sequence which demonstrated peak arterial opacification of the RPA was subtracted from the sequence demonstrating peak venous opacification of the RSPV. The rationale behind choosing these two specific anatomical locations was to ensure that maximal opacification of the pulmonary veins was achieved by ensuring there was maximal subtraction of contrast from the PA system.

Qualitative MR image analysis

The two readers were provided with the conventional TWIST sequence and the novel subtracted TWIST data sets in source and MIP (50 mm thickness) coronal reformats. The subjective quality of the 4 datasets were independently evaluated by two Radiologists (LL and JM; both with 20 years' experience in cardiovascular imaging respectively) using a PACS monitor with 5-megapixel resolution (Barco®), blinded to the imaging protocol and to each others' scores. Each reader was asked to review the 4 sequences in the coronal acquisition: the source TWIST, novel subtracted TWIST, MIP TWIST and novel

subtracted MIP TWIST. An average score for the visualization of the pulmonary veins, pulmonary ostia and left atrium was calculated using a 1–5 scoring methodology adapted from a prior study [4] as follows: (1) non-diagnostic, (2) poor, (3) moderate, (4) good and (5) excellent (Table 1). Scoring examples are provided in Figs. 1, 2 and 3. The indication for the cardiac MRI, underlying congenital cardiac disease and prior cardiac surgery was available at the time of analysis.

Objective quantitative image analysis

A region of interest of 100 pixels was used for all patients. The ROI was placed over the RSPV on the coronal source and novel subtracted TWIST images to quantify the signal intensity (SI). An additional ROI of the same size was placed outside the body in air for background noise measurement. SNR for each sequence was defined as the ratio of mean SI_{RSPV} to the standard deviation of background noise (SI_{AIR}).

Statistical analysis

A Student’s t-test was used for comparison of the mean visualization score of the pulmonary veins and left atrium between the source TWIST and novel subtracted TWIST images, and also between the MIP TWIST and novel subtracted MIP TWIST images. The intra-class correlation coefficient (ICC) was used to determine inter-observer reliability, using a two way mixed approach. Comparison of paired SNR values was performed using the Wilcoxon signed rank test. SPSS was used for statistical analysis. A p value ≤ 0.05 was considered statistically significant for all statistical tests.

Results

Image acquisition

All 21 consecutive patients successfully completed their cardiac MRI study. 1 patient was excluded due to a non-diagnostic study secondary to severe motion artifact. All

Table 1 Assessment of visualization of the PVs and LA using 5-point criteria

Image quality score	Visualization of the PVs and LA	Presence of artifacts	Diagnostic value
1. Non-diagnostic	PVs and LA not visualized	Massive artifacts, non-diagnostic images	No diagnosis possible
2. Poor	Poor visualization of the PV lumen PV vessel edge Smallest branches of the PV Poor distinction between branches of the PV and PA Poor visualization of LA	Moderate artifacts, diagnostic content precarious	Poor, doubt on the diagnosis owing to poor image quality
3. Moderate	Moderate visualization of the PV lumen PV vessel edge Smallest branches of the PV Moderate distinction between branches of the PV and PA Moderate visualization of LA	Moderate artifacts, diagnostic content interfered	Moderate, diagnosis of primary findings only inconclusive
4. Good	Good visualization of the PV lumen PV vessel edge Smallest branches of the PV Good distinction between branches of the PV and PA Good visualization of LA	Mild artifacts, diagnostic content not interfered	Good, still diagnostic, secondary findings not definitively ascertained
5. Excellent	All PVs visualized Excellent visualization of the PV lumen PV vessel edge Smallest branches of the PV Excellent distinction between branches of the PV and PA Excellent visualization of LA	No artifacts	Excellent, fully diagnostic

PV pulmonary vein, PA pulmonary artery, LA left atrium

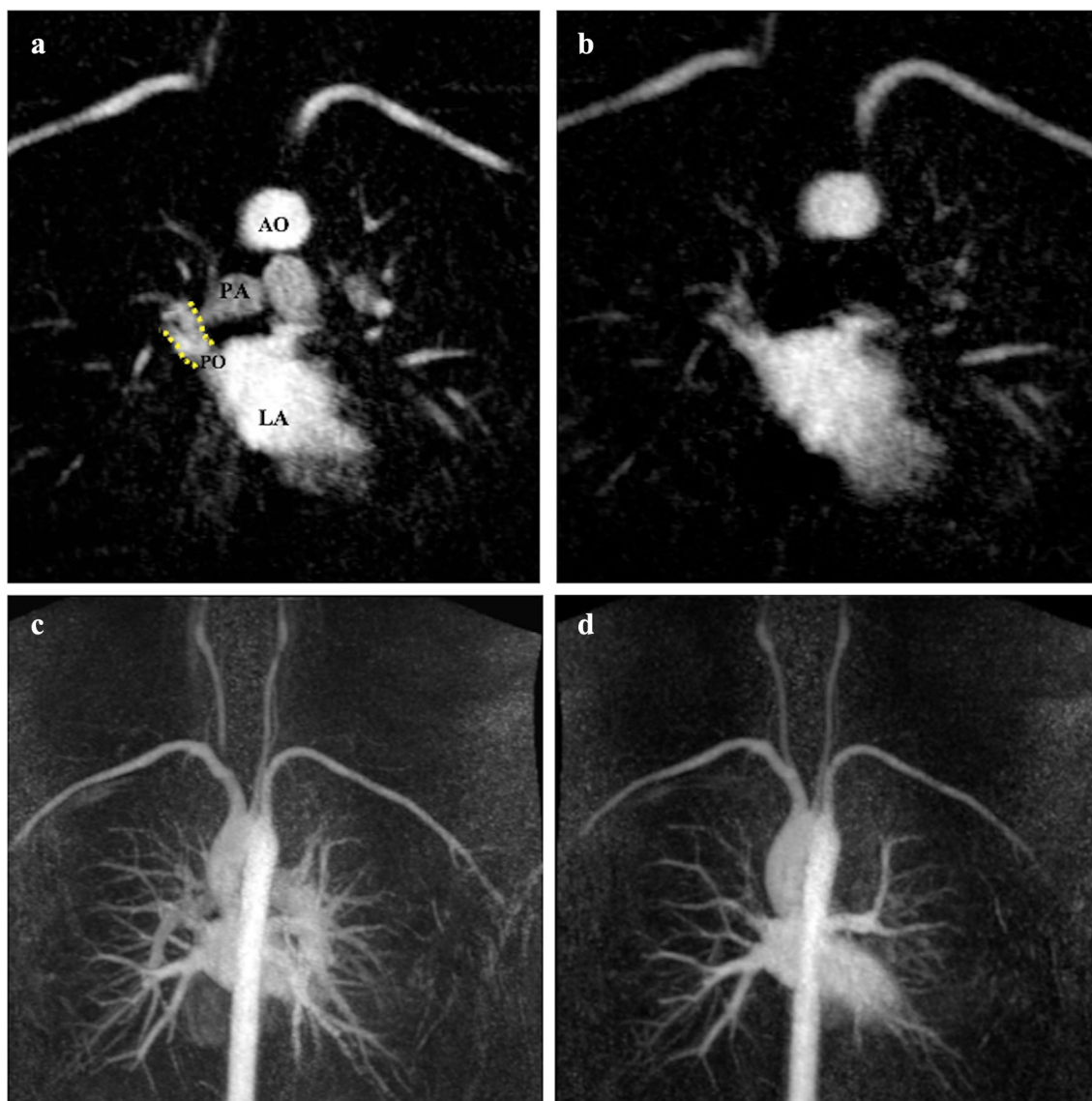


Fig. 1 38-year-old female with TOF and prior surgical correction. **a** Annotated source coronal TWIST image demonstrates synchronous opacification of the right PA and RSPV (dotted yellow lines). In this case the RSPV and left atrium was judged a visualization score of 2 and 4 respectively. **b** Post subtraction, the subtracted coronal TWIST improved visualization of the RSPV by removing contrast within the pulmonary arteries. The RSPV and left atrium were both judged a score of 4. **c** and Video 1: Coronal MIP TWIST sequence demon-

strates simultaneous contrast enhancement of the all cardiac chambers, aorta, pulmonary artery and veins, limiting detailed evaluation of the pulmonary veins. The RSPV was judged a score of 2 and left atrium a score of 4. **d** and Video 2: Coronal subtracted MIP TWIST shows excellent delineation of all pulmonary veins. The RSPV, all pulmonary veins and the LA were judged a score of 5. *TOF* tetralogy of fallot, *AO* aorta, *PA* pulmonary artery, *PO* pulmonary ostium, *LA* left atrium, *RSPV* right superior pulmonary vein

data sets were complete and evaluated. The contrast agent was administered without complication.

Qualitative analysis

The subtraction technique demonstrated improved visualization of the pulmonary veins and left atrium in 16/20 (80%) of patients. The overall visualization of pulmonary veins and left atrium was rated on average better for the

novel subtracted TWIST sequence with a mean score of 3.34 ± 0.69 compared to the source TWIST technique with a mean score of 2.92 ± 0.69 (Table 2). This value was statistically significant ($p < 0.008$). Further improvement in the overall visualization of the pulmonary veins and left atrium was achieved with MIP reconstructions. The subtracted MIP TWIST sequence was judged the best overall sequence with mean score of 4.43 ± 0.80 improving from

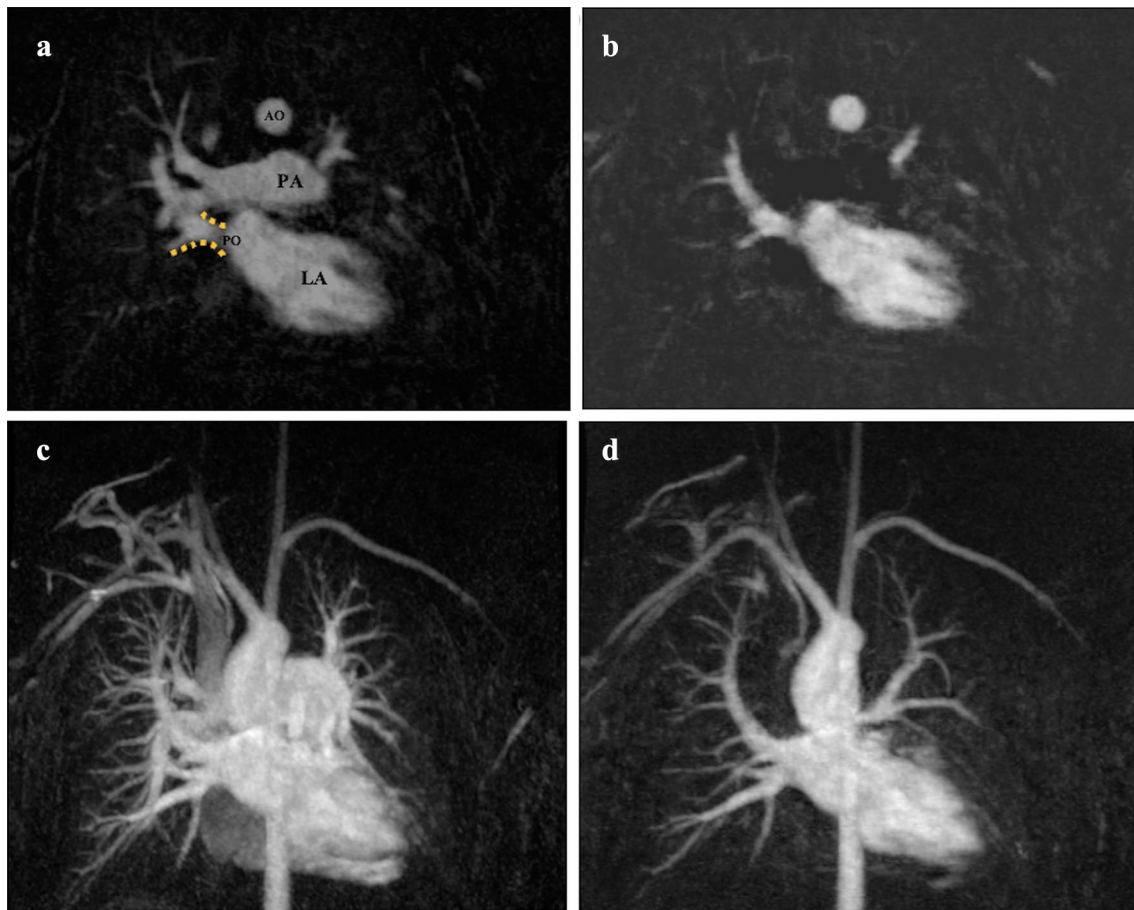


Fig. 2 36-year-old male with TOF and prior corrective surgery. **a** Annotated source coronal TWIST image demonstrates poor distinction between the RSPV (dotted yellow lines). The RSPV was judged a visualization score of 2, left atrium score of 3. **b** Post subtraction, the subtracted coronal TWIST improved visualization of the RSPV by removing contrast within the pulmonary arteries. The RSPV and LA was judged a score of 4. **c** Coronal MIP TWIST sequence demonstrates simultaneous contrast enhancement of the all cardiac cham-

bers, aorta, pulmonary artery and veins, limiting evaluation of the pulmonary veins. Collateral vessels surrounding the right subclavian are noted. The RSPV was judged a score of 2 and the LA a score of 3. **d** Coronal subtracted MIP TWIST shows excellent delineation of all pulmonary veins. The RSPV, all pulmonary veins and the LA were judged a score of 5. *TOF* tetralogy of fallot, *AO* aorta, *PA* pulmonary artery, *PO* pulmonary ostium, *LA* left atrium, *RSPV* right superior pulmonary vein

a mean score of 3.02 ± 0.87 for the MIP TWIST. The difference was statistically significant ($p < 0.001$).

4/20 (20%) patients did not demonstrate improved visualization of the pulmonary veins and left atrium using our outlined subtraction technique. Within this cohort the overall mean score for visualization of the pulmonary veins and left atrium was just above moderate (3.25 ± 0.43). In these four cases, no benefit was acquired as the source TWIST images already had demonstrated at least moderate distinction between the pulmonary veins, for example in Fig. 3, without the need for post-processing subtraction.

The ICC demonstrated good to excellent correlation between the two readers for the 4 sequences yielding values of 0.99 (95% confidence interval 0.983–0.998) for the source TWIST sequence, 0.86 (95% confidence interval 0.652–0.946) for the subtracted TWIST sequence, 0.94 (95% confidence

interval 0.841–0.975) for the MIP TWIST and 1.0 for the subtracted MIP TWIST.

Quantitative analysis

SNR comparisons between the source TWIST and novel subtracted TWIST images demonstrated a minimal reduction in the SNR between the source and subtracted group (85.4 ± 51.1 vs. 70.4 ± 37.4) which was not statistically significant ($p = 0.57$).

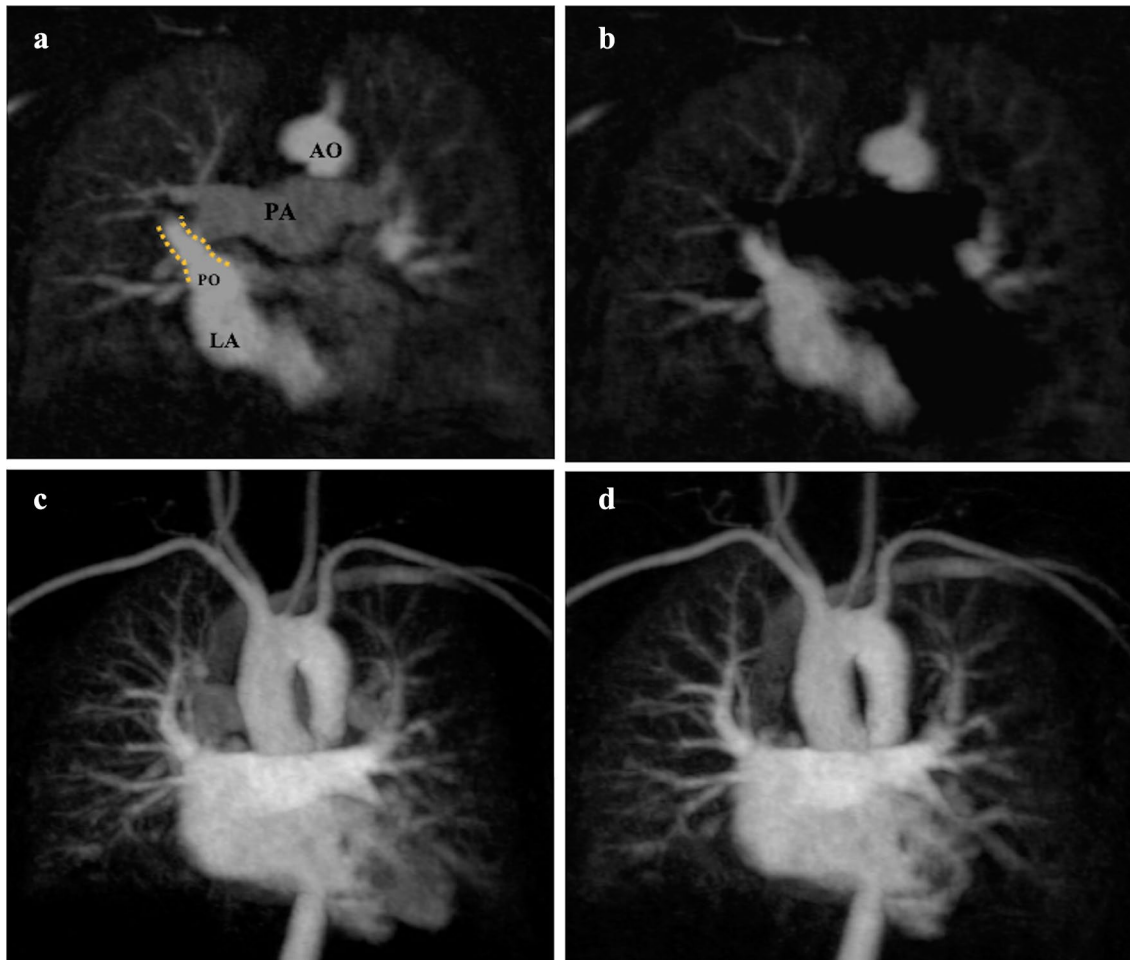


Fig. 3 26-year-old female with history of TGA and Senning procedure providing systemic venous return to the left atrium. **a** Conventional TWIST image demonstrating good visualization of the left atrium and RSP, with both judged a visualization score of 4. **b** Post subtraction, the subtracted coronal TWIST removes contrast within the RV and PA, however does not result improvement the visualization of the LA or PVs. The LA and RSPV was judged a score of 4. **c**

Coronal MIP TWIST demonstrates good visualization of the all pulmonary veins and LA (Score 4). **d** Coronal subtracted MIP TWIST demonstrates no significant improvement post subtraction (Score 4). *TGA* transposition of great arteries, *AO* aorta, *PA* pulmonary artery, *PO* pulmonary ostium, *LA* left atrium, *RSPV* right superior pulmonary vein

Table 2 Overall visualization scores of the pulmonary veins and left atrium (mean \pm SD) in 20 patients undergoing TR-MRA using the TWIST sequence

Sequence	Conventional TWIST	Novel subtracted TWIST	p value
Source	2.92 \pm 0.69	3.34 \pm 0.69	<0.008
MIP	3.02 \pm 0.87	4.43 \pm 0.80	<0.001

Discussion

Our novel post-processing subtraction technique in both source and MIP reformats demonstrated superior visualization of the pulmonary veins and left atrium compared

to the conventional source TWIST and MIP images. The novel subtracted MIP TWIST images were judged the best method for visualization of the PVs and LA.

Clinical relevance

CHD patients frequently demonstrate complex vascular anatomy, cardiac shunts and post-surgical cardiac anatomy which generates dynamic changes in blood flow. Consequently, right and left sided cardiac chambers and cardiac vessels can enhance simultaneously creating a vascular overlay that can limit evaluation of individual cardiovascular structures. TR-MRA has significantly overcome this limitation by providing dynamic hemodynamic flow information [7]. Our described subtraction technique embraces the time

resolved nature of the TWIST sequence to provide a useful adjunct in the evaluation of left heart structures, in particular the pulmonary veins and left atrium through subtraction of contrast from within the right side of the heart (Figs. 1, 2, Video 1 and 2). The incorporated videos aim to provide the reader with a 3D view of the relationship between the pulmonary vasculature and left atrium, which is not as evident on the static single slice images. The focus of this study was not to assess visualization of the right heart structure (superior vena cava, right atrium, right ventricle and pulmonary arteries). Typically these structures are the first to enhance on the early TWIST sequences and frequently well visualized without superimposed opacification of the left sided cardiopulmonary structures.

Time resolved sequence in cardiac MRI

Time-resolved contrast-enhanced techniques were initially used in the assessment of thoracic, abdominal, and peripheral blood vessels [8–10]. Time resolved techniques provide anatomical and dynamic flow information, and now currently employed in the evaluation patients with complex congenital heart disease [11]. The key principle of time resolved MRI is based on under sampling of k-space [12]. During image acquisition after administration of IV contrast, the center of k-space is sampled more frequently than the periphery. Thus, the missing data can be manipulated to generate a full k-space data set to create time resolved images with acceptable spatial resolution. A range of time-resolved imaging techniques have described including keyhole [13, 14], time-resolved imaging of contrast kinetics (TRICKS) [15], time-resolved echo-shared angiographic technique [16] (TREAT), block regional interpolation scheme for K-space (BRISK) [17], continuous updating with random encoding (CURE) [18] to name a few. Recently, compressed sensing time-resolved imaging with stochastic trajectories [19] (CS-TWIST) shows promise as a technique to reduce temporal and spatial blurring artifacts inherently associated with time-resolved sequences. In conjunction with the introduction of 3T field strength magnets, which improves SNR while maintaining contrast to noise [20], time-resolved sequences are now well established in cardiac MRI protocols.

Clinical implications of the subtracted time-resolved TWIST sequence

This novel subtracted TWIST sequence we have described utilizes images acquired in a conventional TWIST data set in a patient undergoing a routine outpatient cardiac MRI. It does not require additional sequences, a prolonged scan time, a higher dose of intravenous contrast or additional software. While the subtraction of images requires an increased post-processing time (approximately 10 min

and initial learning curve, we have demonstrated that it significantly improves visualization of pulmonary veins and left atrium in a substantial number of patients. Recent studies [5, 6] have demonstrate that TR-MRA provide superior visualization of the pulmonary veins compared to contrast enhanced MRA (CE-MRA). Our post-processing technique would serve as a useful adjunct in patients undergoing TR-MRA for evaluation of pulmonary venous anomalies [21–23]. This novel subtraction technique could also be used as a non-ionizing alternative to cardiac CT in patients with atrial fibrillation to facilitate the use of electro-anatomical mapping systems at the time of ablation procedures. Subtracted cardiac MRI images can provide detailed pre-procedural anatomical imaging, in particular to identify PVs and LA anatomical variation, which can be imported into the 3D electrophysiological mapping system to increases ablation success and reduces complication rates [24–26].

Limitations

Our study population included a broad spectrum of CHD, and did not evaluate a specific subtype of CHD, for example cyanotic vs acyanotic or surgically corrected vs non-corrected. We feel this reflects the significant variation in CHD we encounter in our day-to-day practice. Secondly, the study did not account for physiological parameters that can alter flow hemodynamics such as shunts, baffles or right and left ventricle ejection fraction. Thirdly, assessment of the impact of the subtraction technique on diagnosis or radiological findings was not performed. We feel this analysis would be of particular value in patients with pulmonary venous anomalies and pre- and post pulmonary vein ablation procedures and is of interest for further study. A further limitation of the study is the small sample size. Finally, although both readers were blinded to the imaging protocol, in certain studies it was evident when the novel subtraction technique had been applied, as a region of homogenous hypointensity was seen in the expected location of the subtracted pulmonary artery (Images 1B, 2B and 3B).

Conclusion

Compared with source TR-MRA images, subtraction of TR-MRA images is a novel post-processing technique that improves visualization of the pulmonary veins and left atrium in a substantial number of patients.

Compliance with ethical standards

Conflict of interest The authors declared that they have no conflict of interest.

References

- Foster E, Graham TP Jr, Driscoll DJ et al (2001) Task force 2: special health care needs of adults with congenital heart disease. *J Am Coll Cardiol* 37:1176–1183
- Lane DA, Lip GY, Millane TA (2002) Quality of life in adults with congenital heart disease. *Heart* 88:71–75
- Fenchel M, Saleh R, Dinh et al (2007) Juvenile and adult congenital heart disease: time-resolved 3D contrast-enhanced MR angiography. *Radiology* 244:399–410
- Vogt FM, Theysohn JM, Michna D et al (2013) Contrast-enhanced time-resolved 4D MRA of congenital heart and vessel anomalies: image quality and diagnostic value compared with 3D MRA. *Eur Radiol* 23:2392–2404
- Schonberger M, Usman A, Galizia M et al (2013) Time-resolved MR venography of the pulmonary veins pre-catheter-based ablation for atrial fibrillation. *J Magn Reson Imaging* 37:127–137
- Zghaib T, Shahid A, Pozzessere C et al (2018) Validation of contrast-enhanced time-resolved magnetic resonance angiography in pre-ablation planning in patients with atrial fibrillation: comparison with traditional technique. *Int J Cardiovasc Imaging* 16:1–8
- Song T, Laine AF, Chen Q et al (2009) Optimal k-space sampling for dynamic contrast-enhanced MRI with an application to MR renography. *Magn Reson Med* 61:1242–1248
- Finn JP, Baskaran V, Carr JC et al (2002) Thorax: low-dose contrast-enhanced three-dimensional MR angiography with sub-second temporal resolution—initial results. *Radiology* 224:896–904
- Van Hoe L, De Jaegere T, Bosmans H et al (2000) Breath-hold contrast-enhanced three-dimensional MR angiography of the abdomen: time-resolved imaging versus single-phase imaging. *Radiology* 214:149–156
- Swan JS, Carroll TJ, Kennell TW (2002) Time-resolved three-dimensional contrast-enhanced MR angiography of the peripheral vessels. *Radiology* 225:43–52
- Driessen MM, Breur JM, Budde RP et al (2015) Advances in cardiac magnetic resonance imaging of congenital heart disease. *Pediatric Radiol* 45(1):5–19
- Tsao J, Kozerke S (2012) MRI temporal acceleration techniques. *J Magn Reson Imaging* 36:543–560
- Riederer SJ, Tasciyan T, Farzaneh F et al (1988) MR fluoroscopy: technical feasibility. *Magn Reson Med* 8:1–15
- van Vaals JJ, Brummer ME, Dixon WT et al (1993) ‘‘Keyhole’’ method for accelerating imaging of contrast agent uptake. *J Magn Reson Imaging* 3:671–675
- Korosec FR, Frayne R, Grist TM et al (1996) Time-resolved contrast-enhanced 3D MR angiography. *Magn Reson Med* 36:345–351
- Fink C, Ley S, Kroeker R et al (2005) Time-resolved contrast-enhanced three-dimensional magnetic resonance angiography of the chest: combination of parallel imaging with view sharing (TREAT). *Invest Radiol* 40:40–48
- Doyle M, Walsh EG, Blackwell GG et al (1995) Block regional interpolation scheme for k-space (BRISK): a rapid cardiac imaging technique. *Magn Reson Med* 33:163–170
- Parrish T, Hu X (1995) Continuous update with random encoding (CURE): a new strategy for dynamic imaging. *Magn Reson Med* 33:326–336
- Rapacchi S, Natsuaki Y, Plotnik A (2015) Reducing view-sharing using compressed sensing in time-resolved contrast-enhanced magnetic resonance angiography. *Magn Reson Med* 74:474–481
- Hinton DP, Wald LL, Pitts J et al (2003) Comparison of cardiac MRI on 1.5 and 3.0 T clinical whole body systems. *Invest Radiol* 38:436–442
- Prompona M, Muehling O, Naebauer M et al (2011) MRI for detection of anomalous pulmonary venous drainage in patients with sinus venosus atrial septal defects. *Int J Cardiovasc Imaging* 27:403–412
- Ferrari VA, Scott CH, Holland GA et al (2001) Ultrafast three-dimensional contrast-enhanced magnetic resonance angiography and imaging in the diagnosis of partial anomalous pulmonary venous drainage. *J Am Coll Cardiol* 37:1120–1128
- Festa P, Ait-Ali L, Cerillo AG et al (2006) Magnetic resonance imaging is the diagnostic tool of choice in the preoperative evaluation of patients with partial anomalous pulmonary venous return. *Int J Cardiovasc Imaging* 22:685–693
- Deshmukh A, Patel NJ, Pant S et al (2013) In-hospital complications associated with catheter ablation of atrial fibrillation in the United States between 2000 and 2010: analysis of 93 801 procedures. *Circulation* 128:2104–2112
- Kistler PM, Rajappan K, Jahngir M et al (2006) The impact of CT image integration into an electroanatomic mapping system on clinical outcomes of catheter ablation of atrial fibrillation. *J Cardiovasc Electrophysiol* 17:1093–1101
- Ghaye B, Szapiro D, Dacher JN, Rodriguez et al (2003) Percutaneous ablation for atrial fibrillation: the role of cross-sectional imaging. *Radiographics* 23(suppl_1):S19–S33

Publisher’s Note Springer Nature remains neutral with regard to jurisdictional claims in published maps and institutional affiliations.